pH–Dependent Interactions Between Lead and Typha angustifolia Biomass in the Biosorption Process

4 AUTHORS, INCLUDING:

Hong Jiang
University of Science and Technology of China
55 PUBLICATIONS **647** CITATIONS

SEE PROFILE

Han-Qing Yu
University of Science and Technology of China
508 PUBLICATIONS **11,036** CITATIONS

SEE PROFILE

pH-Dependent Interactions Between Lead and *Typha angustifolia* Biomass in the Biosorption Process

Wu-Jun Liu,[†] Fan-Xin Zeng,[†,‡] Hong Jiang,[*,†] and Han-Qing Yu[†]

[†]Department of Chemistry, University of Science and Technology of China, Hefei 230026, P.R. China

[‡]Key Laboratory of Cellulose and Lignocellulosics Chemistry, Guangzhou Institute of Chemistry, Chinese Academy of Sciences, Guangzhou 510650, P.R. China

Ⓢ *Supporting Information*

ABSTRACT: Removal of heavy metals from wastewater by biosorption is an attractive approach. In this work, the interactions between lead and *Typha angustifolia* biomass, a cost-effective biosorbent, were investigated. It was found that the interactions between lead and *T. angustifolia* biomass were complex, and the solution pH was a key factor governing such interactions. The FTIR characterization and the results of blocking experiment indicate the amino, hydroxyl, and carboxyl are the main functional groups contributing to these interactions. A synergistic mechanism involving ion exchange, complexation, and hydrogen binding was elucidated. According to this mechanism, the dominant interactions between the biomass and lead altered with the variation of pH, which was consistent with the experimental results. Additionally, a simple method was explored to estimate the contributions of different interactions between the biomass and lead.

1. INTRODUCTION

Heavy metals have caused serious environmental problems as they are extremely harmful to humans, animals, and plants because of their toxicity, accumulation, and nonbiodegradable nature. Among these, lead is one of the most ubiquitously spread heavy metals because of several thousand years of use. Industrial activities such as microelectronics, electroplating, battery manufacture, and metallurgy are considered as the major sources of lead release into the environment.[1,2] It is well verified that lead can cause adverse health effects including neurotoxicity, nephrotoxicity, and deleterious effects on the hematological and cardiovascular systems.[3]

Biosorption is a promising technology for the treatment of heavy metal polluted wastewater because of its advantages of high efficiency and low cost. Many plant biomasses have great metal binding capacity and are widely used in the removal of heavy metals from wastewater.[4−7] *Typha angustifolia*, an extensively used plant in constructed wetland in recent years for the removal of pollutants, is produced in a large quantity every year.[8−11] However, when in a decline phase, the plant biomass wilts and decays, and the pollutants in the biomass are released to the wetland system again, causing a secondary pollution.[12,13] Considering the high amino acid and polysaccharide (the compounds rich in carboxyl, amino, and hydroxyl groups) contents,[14] one of prospective methods to avoid this secondary pollution is to employ the *T. angustifolia* biomass to treat heavy metal contaminated wastewater. Many recent studies indicate that chemical interactions between metal ions and the functional groups on the biomass surface, such as carboxyl, hydroxyl, phosphate, sulfate, and amino groups, are the primary driving force in the removal of heavy metals by the biomass.[15−17] Among them, ion-exchange is considered by many researchers as a dominant interaction between the functional groups and the metals[18−21] which can interpret well the experimental results at low pH value. Nevertheless, the experimental results are usually inconsistent with the ion-exchange mechanism in the adsorption system without ionic

state metals (the metals appearing in hydroxides or the complexation state).[22] Fourest and Volesky[23] pointed out that the surface complexation also existed in metal binding with the biomass functional groups, and other researchers verified the mechanism of surface complexation.[24−26] Actually, the species of heavy metals in the solution often change with the variation of pH value; thus, the chemical interactions between heavy metals and functional groups are very complex. In addition to the ion-exchange and complexation, other pH-dependent interactions (e.g., hydrogen binding or the synergetic effects among ion-exchange, complexation, and hydrogen binding) should also be taken into account. Few attempts have been made to explore the pH-dependent interactions between the biomass functional groups and heavy metals.

The objective of this work is to investigate the pH-dependent interactions between lead and the *T. angustifolia* biomass in the biosorption process. The influence of the lead species' changes caused by variation of the initial solution pH on the lead uptake capacity was described. A synergistic mechanism involving ion exchange, complexation, and hydrogen binding was proposed to illuminate the lead uptake process at different pH values. Additionally, scanning electron microscopy energy dispersive X-ray (SEM-EDX) and FTIR characterizations of the *T. angustifolia* biomass before and after lead uptake were performed to analyze the changes of the biomass during the chemical interaction process.

2. MATERIALS AND METHODS

2.1. Materials. Reagents in this work were of analytical grade and purchased from Sinopharm Chemical Reagent Co., Ltd.,

Table 1. General Characteristics and Constituents of the Biomass

proximate analysis (wt %)		ultimate analysis (wt %)	
moisture	4.42	C	42.30
volatile matter	72.02	H	5.69
fix carbon	17.05	N	2.93
ash	10.93	P	0.58
density(g cm^{-3})	0.99	O^a	48.50

^{a} By difference.

Shanghai, China. A stock solution of 1000 mg L^{-1} of lead was prepared by dissolving a desired amount of Pb(NO$_3$)$_2$ in deionized water and making the volume up to 1000 mL in a brown volumetric flask. A series of work solutions with the concentrations ranging from 20 to 600 mg/L of lead were prepared by appropriate dilution of the stock solution immediately prior to their use.

T. angustifolia biomass was collected randomly from a wetland located in University of Science and Technology of China (31°49′59″ E, 117°15′54″ N). After harvest, it was washed several times with deionized water to remove the dust particles, and then dried in an oven at 378 K for 24 h. The dried biomass was crushed by a high-speed rotary cutting mill, and the particles with the size between 0.15 mm and 0.30 mm were collected and stored in a glass container for the experiments.

The proximate analysis of the biomass was referred to ASTM Standard Test Method D5142, and the ultimate analysis was carried out using an elemental analyzer (VARIO EL III, Elementar, Germany). The general characteristics and constituents of the biomass are listed in Table 1. The thermal stability of the biomass (see Supporting Information, Figure S1) was characterized with a DTG-60H/DSC-60 thermogravimetric analyzer (Shimadzu, Japan). Structural features of the biomass were obtained from nitrogen adsorption–desorption isotherms (see Supporting Information, Table S1), carried out at 77 K using a Micromeritics Gemini apparatus (ASAP 2020 M+C, Micromeritics. Co. U.S.A.). Specific surface area was obtained by the Brunauer–Emmett–Teller (BET) method, and total pore volume was calculated by the amount of nitrogen adsorbed at a relative pressure of 0.97 (see Supporting Information, Figure S2).

2.2. Biosorption Experiments. The adsorption experiments of the *T. angustifolia* biomass were carried out in 250 mL conical flasks at 298 K. A 0.3 g portion of biomass and 100 mL of Pb (II) solution in the desired concentration were mixed in the flasks and shaken in a constant-temperature oscillator (WHY-2, China) with an oscillation frequency of 200 rpm. The initial solution pH ranging from 2.0 to 8.0 was adjusted to the desired value by adding a small quantity of 1.0 mol L^{-1} HNO$_3$ or 1.0 mol L^{-1} NaOH, and measured with a pH meter (PHS-25, China). After the adsorption, the suspension liquids were separated by filtration through a membrane filter (0.45 μm). The concentration of lead in the filtrate was determined by an inductively coupled plasma-atomic emission spectrometry (ICP-AES) (Optima 7300 DV, Perkin-Elmer Corporation, U.S.A.). The Pb-loaded biomass was dried at 378 K for 24 h, and then stored in a glass bottle for further use. Lead removal efficiency (R) was calculated from eq 1:

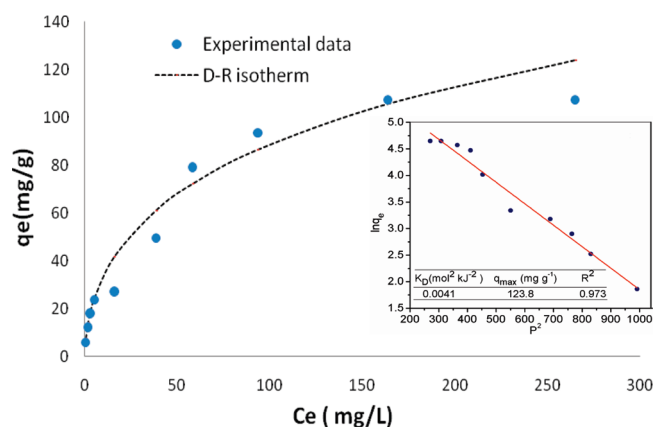$$R = \frac{C_0 - C_e}{C_0} \times 100\% \tag{1}$$

Figure 1. Adsorption isotherm of lead on the biomass with different lead concentrations; (Inset figure), Fitting of the D-R model. Adsorption conditions: initial pH, 6.0; initial lead concentration, 20−600 mg L^{-1}; contact time, 300 min; biomass dosage, 3.0 g L^{-1}; temperature, 298 K.

where C_0 (mg L^{-1}) and C_e (mg L^{-1}) are initial and equilibrium lead concentrations, respectively.

The amount of lead adsorbed by the biomass was calculated using the eq 2:

$$q_e = \frac{(C_0 - C_e) \times V}{w} \tag{2}$$

where q_e (mg g^{-1}) is the adsorption capacity of the biomass at equilibrium, w (g) is the adsorbent dosage, and V (L) is the volume of the solution.

2.3. FTIR, SEM-EDX Analysis of Original and Pb-Loaded Biomass. The Pb-loaded biomass was obtained by shaking 0.3 g of original biomass with 100 mL of 100 mg L^{-1} lead(II) solution at pH 6.0 for 300 min. The original and Pb-loaded biomass were mixed with KBr at a ratio of 1:100 and compressed into films, respectively. The films were characterized using Fourier transformed infrared spectroscopy (FTIR, EQUIVOX55 IR spectroscopy, Bruker, Germany). The surface morphology and microarea chemical composition of the original and Pb-loaded biomass were analyzed by scanning electron microscope (SEM, XL-30 ESEM, FEI electron optics company, U.S.A.) coupled with energy dispersive X-ray (EDX) spectrometer.

3. RESULTS AND DISCUSSION

3.1. Adsorption Isotherm. Lead adsorption capacities of *T. angustifolia* at different initial concentrations are presented in Figure.1. The experimental data were evaluated using Dubinin–Radushkevich isotherm model (D-R model), which is widely employed to check the nature of the adsorption as physical or chemical process.[27] This model can be described by eqs 3 and 4:

$$q_e = q_{max} \exp\left(-K_D\left[RT\ln\left(1+\frac{1}{c_e}\right)\right]^2\right) = q_{max}\exp(-K_D P^2) \tag{3}$$

$$\ln q_e = \ln q_{max} - K_D P^2 \tag{4}$$

where $P = RT\ln(1+(1/c_e))$ is the polar potential, $R = 8.314 \times 10^{-3}$ (kJ mol^{-1} K^{-1}) is the universal gas constant, T (K) is the temperature. K_D (mol^2 kJ^{-2}) is the constant related to the mean
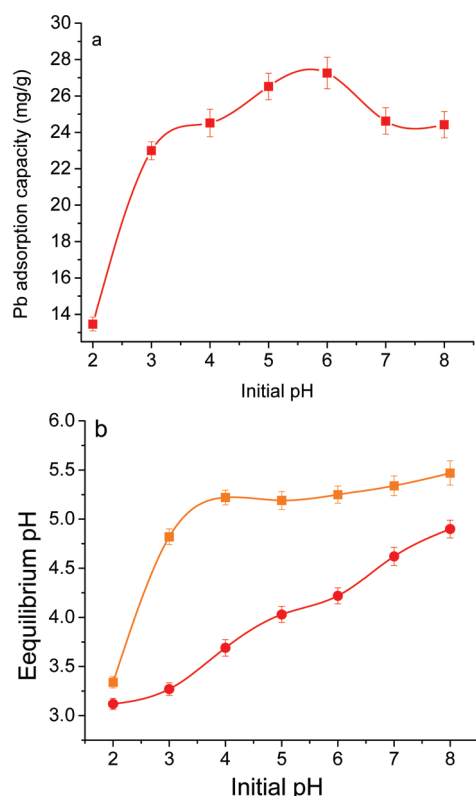
Figure 2. (a) Effect of pH on the lead adsorption capacity of *T. angustifolia*; (b) Changes of the pH values in the adsorption process (red solid circles control test, 3.0 g L^{-1} of biomass in 100 mL deionized water; orange solid squares 3.0 g L^{-1} of biomass in 100 mg L^{-1} of lead solution).

free energy (E). The values of K_D and q_{max} are provided by the slope and intercept of the plot of $\ln q_e$ versus P^2 (Figure 1 inset), and the value of E is calculated using the obtained value of K_D from eq 5:

$$E = \frac{1}{\sqrt{-2K_D}} = 11.07 \ (\text{kJ mol}^{-1}) \qquad (5)$$

When the value of E is in range of $1.0-8.0$ kJ mol^{-1}, the adsorption is considered as a physical adsorption process, and the value of E ranged from 8.0 to 16.0 kJ mol^{-1} indicates a chemical adsorption process.[28] Thus, the adsorption of lead on *T. angustifolia* biomass can be attributed to be a chemical adsorption process according to value of E.

3.2. Effect of pH. Solution pH is a key factor influencing the adsorption process. It not only affects the states of the functional groups on the surface of the biomass, but also the existing form of the metal ions presented in solution. Figure 2a shows the effect of pH on the lead adsorption of *T. angustifolia*. It is observed that the lead adsorption capacity increased from 13.47 to 27.26 mg g^{-1} in the pH range of $2.0-6.0$, showing a maximum value at pH 6.0. With further increase in pH to 7.0 and 8.0, the adsorption capacity slightly decreased to 24.62 and 24.42 mg g^{-1}. A similar phenomenon was also reported by other researchers.[2,29]
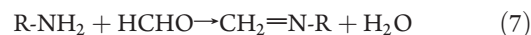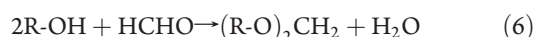
Figure 2b shows the change of pH value in the adsorption process. To investigate the effect of biomass itself on the pH changes, a control test was carried out by shaking 0.3 g of biomass in 100 mL of deionized water at different initial pH. Under low pH condition (pH 2.0 to 5.0), the equilibrium pH is higher than the initial pH. It can be interpreted that the functional groups (mainly amino and hydroxyl groups) absorbed some H$^+$ ions to form protonated groups. While at high initial pH, the equilibrium pH is decreased, showing that some more functional groups are deprotonated, releasing H$^+$ ions to the solution.

3.3. Study of the Adsorption Mechanism. *3.3.1. SEM-EDX and FTIR Characterization of the Biomass.* SEM-EDX has been widely used for the analysis of the surface microstructures and microarea chemical composition of the biomass so as to elucidate the probable mechanism of adsorption. The SEM micrographs and EDX spectra of the original and Pb-loaded biomass are presented in Figure.3a. The micrographs reveal that the biomass has a typical fibrous structure. There are some small lead-enriched particles on the surface of the biomass after adsorption, which is confirmed by the EDX spectra.

To determine the main functional groups of the biomass participating in lead adsorption, the original and Pb-loaded biomass were characterized using FTIR. On the basis of the analysis of IR spectra (Figure 3b), the band positions for the function groups are listed in Table 2. Comparing to the peak at 3407 cm^{-1} for the original biomass, the vibration of the hydroxyl and/or amino group for the Pb-loaded biomass shifted significantly to 3423 cm^{-1}, indicating the involvement of hydroxyl and/or amino group in the adsorption of lead. Another significantly shifted peak is attributed to the stretching of the C=O in the carboxyl groups, which shifted from 1640 cm^{-1} to 1630 cm^{-1} after the adsorption process. It likely results from the change of the existence form of the carboxylic groups during the adsorption process. No obvious shift was observed for other peaks except the peaks discussed above. Accordingly, the hydroxyl, amino, and carboxyl groups on the surface of the biomass might be the main functional groups involved in lead adsorption.

3.3.2. Contributions of Functional Groups to the Lead Adsorption. To further investigate the contributions of the functional groups in the adsorption of lead, the hydroxyl/amino and carboxyl groups were blocked by chemical methods, respectively. The blocking of the hydroxyl and amino groups was carried out according to the following reactions:[30,31]

$$2\text{R-OH} + \text{HCHO} \rightarrow (\text{R-O})_2\text{CH}_2 + \text{H}_2\text{O} \qquad (6)$$

$$\text{R-NH}_2 + \text{HCHO} \rightarrow \text{CH}_2=\text{N-R} + \text{H}_2\text{O} \qquad (7)$$

The carboxyl groups were blocked by esterification reaction with methanol at acidic condition (eq 8).[32]

$$\text{RCOOH} + \text{CH}_3\text{OH} \xrightarrow{\text{H}^+} \text{RCOOCH}_3 + \text{H}_2\text{O} \qquad (8)$$

The chemically modified biomass was employed for lead adsorption with initial Pb concentration of 100 mg L^{-1} at pH 6.0, and the equilibrium adsorption capacity is presented in Figure 4. The results show that the adsorption capacity sharply decreases when the functional groups are blocked. When hydroxyl and amino groups are blocked, the adsorption capacity is 17.03 mg g^{-1}, decreasing by 36.70% in adsorption capacity compared to that of the original biomass (26.94 mg g^{-1}). After the blocking of carboxyl groups, the adsorption capacity is decreased to 12.42 mg g^{-1}, which is only 46.14% of the adsorption capacity of the original biomass. The experimental results are in agreement with reported works.[16,17] Therefore, functional groups blocking tests, coupled with the FTIR analysis, indicated that the hydroxyl, amino, and carboxyl groups were mainly responsible for lead adsorption on the *T. angustifolia*.
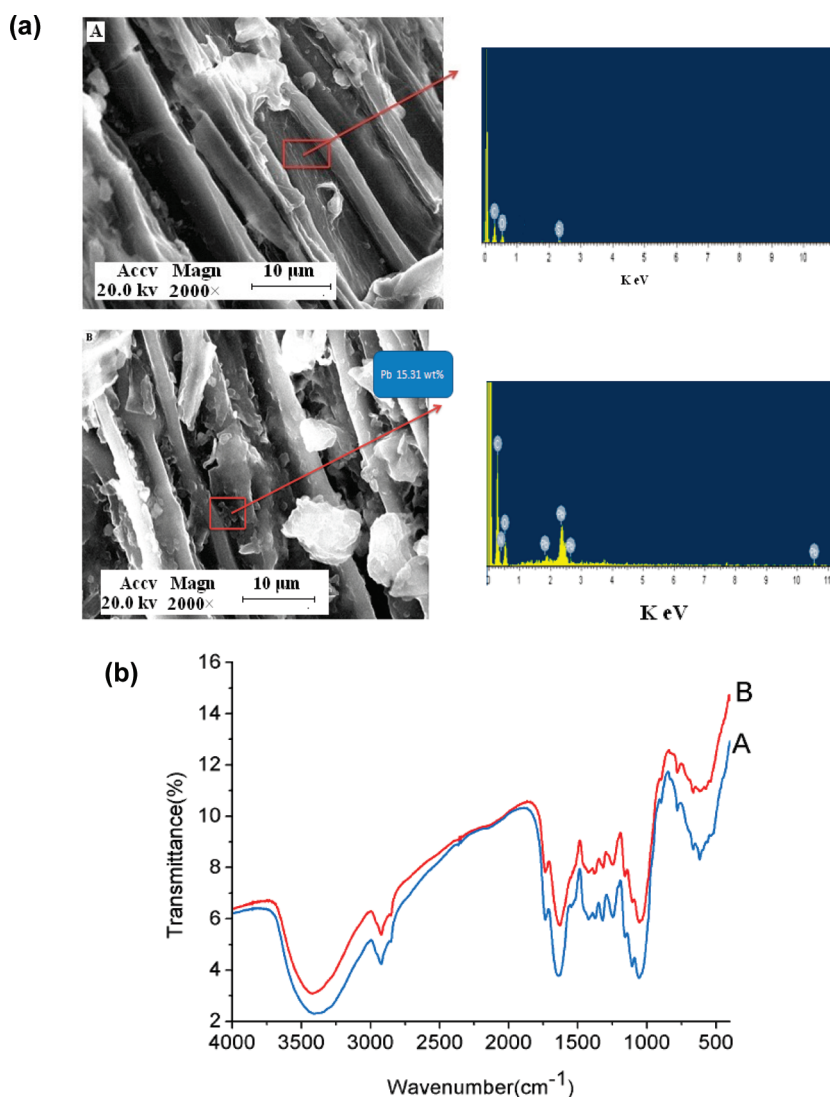
(a)

(b)

Figure 3. (a) SEM-EDX analysis of the biomass, (A) original biomass, and (B) Pb-loaded biomass; (b) FTIR spectra of the biomass, (A) original biomass, and (B) Pb-loaded biomass.

3.3.3. Adsorption Mechanism. As the specific surface area and pore volume of the biomass are very low (see Supporting Information, Table S1), the physical interaction in the lead adsorption process is not appreciable. The lead adsorption of the *T. angustifolia* is mainly attributed to the chemical interaction between lead ions and the functional groups on the surface of the biomass. Ion exchange and complexation mechanisms (eqs 9 and 10) have just been taken into account in the adsorption process during past decades.

$$R^{n-}E^{n+} + M^{n+} \leftrightarrow R^{n-}M^{n+} + E^{n+} \qquad (9)$$

$$M^{n+} + mBL \rightarrow M(BL)_m^{n+} \qquad (10)$$
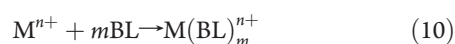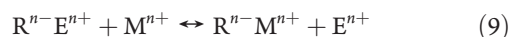
where $R^{n-}E^{n+}$ is the biomass with exchangeable site (usually carboxyl acid or its salt), M^{n+} represents the metal ion, E^{n+} denotes the exchange ion (H^+ or other metal ions), BL signifies the biomass with ligand groups (usually N or O in the amino or hydroxyl groups). Actually, $Pb(OH)^+$ and $Pb(OH)_2$ exist in solution of certain pH, which can form hydrogen bonds with amino and

hydroxyl groups of the biomass. Thus, a synergistic mechanism involving ion exchange, complexation, and hydrogen binding is more reasonable than the reported mechanisms.

It can be drawn from the metal speciation studies[33,34] that lead dominantly exists as Pb^{2+} in an aqueous solution at pH lower than 4.0. As the pH value further increases, the lead hydroxides ($Pb(OH)^+$ and $Pb(OH)_2$ (aq)) start to form in the solution though the Pb^{2+} is still the main species in the solution. While the pH is higher than 6.0, the $Pb(OH)_2$ ($K_{sp} = 1.43 \times 10^{-15}$, the data obtained from Lange's Handbook of Chemistry, 16th ed., 2005) becomes the dominant species in the solution. For pH higher than 8.0, the $Pb(OH)_2$ starts precipitating from the solutions.

As described in Figure 5, the interaction between lead and the functional groups is highly affected by the lead species which depend on the microenvironment of the solution (mainly the pH value). At pH range of 2.0−4.0, the Pb^{2+} is adsorbed on the surface of the biomass mainly by ion exchange (reaction 1) and complexation (reaction 2). Under this condition, the dominantly existent Pb^{2+} ions in the solution can easily exchange with the

Table 2. Band Positions for the Function Groups of Original and Pb-Loaded Biomass

functional groups	band positions (cm^{-1})	
	original biomass	Pb-loaded biomass
OH and/or NH$_2$ stretching	**3407**	**3423**
-CH$_2$ symmetric stretching	2922	2923
-CH$_2$ asymmetric stretching	2851	2850
C=O stretching in ester and/or amide groups	1737	1736
C=O stretching in carboxyl groups	**1640**	**1630**
CH$_2$ bending vibrations	1422	1423
C—N stretching	1321	1316
	1245	1247
C—O stretching	1158	1159
	1057	1055
finger print of —SH, —PO$_4$	780	781
	664	664
	618	620
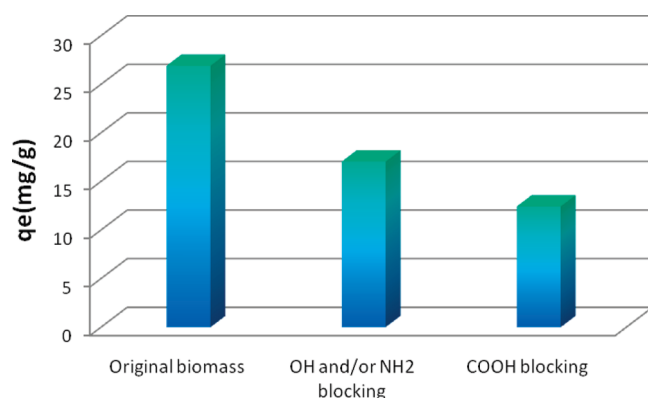
Figure 4. Effect of the functional groups on lead adsorption by *T. angustifoli* biomass. Adsorption conditions: initial pH, 6.0; contact time, 300 min; biomass dosage, $3.0\,g\,L^{-1}$; initial lead concentration, $100\,mg\,L^{-1}$; temperature, 298 K.

protons of the functional groups on the biomass. Meanwhile, the complexation also affects the lead adsorption capacity, which is formed between unoccupied electron orbitals of bivalent lead and lone pair electrons on sp^3 hybridized orbitals of the nitrogen atoms and oxygen atoms of the functional groups. The Pb^{2+} can coordinate with four ligands by sp^{3}d hybridization. On the highly acidic condition, the amino and hydroxyl groups are present in protonated forms (R-NH$_3^+$ and R-OH$_2^+$) which have electrostatic repulsion to the Pb^{2+} and for which it is hard to donate their electron pair to coordinate with Pb^{2+}, thus weakening the complexation between them. With the rising of solution pH, the combined H$^+$ ions gradually dissociate from functional groups, which enhances the complexation between lead and the functional groups.

With a further elevation of pH (4.0—6.0), the adsorption process is more complicated because more lead species (e.g., Pb^{2+}, Pb(OH)$^+$, Pb(OH)$_2$) exist in the solution. Besides the complexation (reaction 2) and ion exchange (reaction 3), the hydrogen binding (reaction 4 and 5) plays an important role in the adsorption. The hydrogen bond is easy to form between the

strongly electronegative oxygen atom in the lead hydroxides and the electron positive hydrogen in the functional groups. The electron positive hydrogen in the lead hydroxides can also form a hydrogen bond with the electronegative oxygen and nitrogen atoms in the functional groups.

In the pH range of 6.0—8.0, the dominant lead species in the solution is Pb(OH)$_2$. The hydrogen binding (reaction 5) and complexation (reaction 6) are the major driving forces in the adsorption, while the ion exchange effect becomes negligible. Considering the weak force of hydrogen binding, whose enhancement cannot counteract the decrease of the ion exchange, the adsorption capacity should decrease to some extent, which is supported by the adsorption experimental results (Figure 2).

In summary, the interaction between lead and the biomass is mainly affected by the lead species which depends on the solution microenvironment (pH).

3.3.4. Estimation of the Contributions of Different Interactions to the Lead Adsorption. Figure 2b shows the equilibrium pH values of control tests are higher than those of Pb adsorption experiments, which indicates that more protons were released to the solution in the lead adsorption process. The effect of other cations in the biomass on H$^+$/Pb^{2+} exchange is not taken into account, the extra release of the protons was mainly attributed to the exchange between protons and lead ions. The amount of lead adsorbed by H$^+$/Pb^{2+} exchange can be calculated on the basis of the amount of protons released to the solution in the exchange process. Equation 11 is put forward to calculate the amount of the lead adsorbed through H$^+$/Pb^{2+} exchange process.

$$q_{\text{ion-exchange}} = \frac{([H^+]_{Pb} - [H^+]_0) \times V \times M_{Pb} \times 1/2}{W} \quad (11)$$

$$\eta_{\text{ion-exchange}} \% = \frac{q_{\text{ion-exchange}}}{q_e} \times 100\% \quad (12)$$

$$[H^+] = 10^{-pH_e} - 10^{-pH_i} \quad (13)$$

where $q_{\text{ion-exchange}}$ is the amount of the lead adsorbed through the H$^+$/Pb^{2+} exchange process, $[H^+]_{Pb}$ and $[H^+]_0$ (mol L^{-1}) are the amounts of protons released in the lead adsorption process and control test, respectively, V (L) is the volume of the solution, M_{Pb}= 207.2 g mol^{-1} is the molar mass of lead, 1/2 is charge ratio of H$^+$ to Pb^{2+}, W (g) is weight of the biomass, q_e (g/g) is the total lead adsorption capacity, $\eta_{\text{ion-exchange}}$ is the proportion of lead adsorbed through ion-exchange process, and pH$_e$ and pH$_i$ are the equilibrium and initial pH values of the solution, respectively.

The contributions of complexation and hydrogen binding to lead adsorption are considered together because they are difficult to subdivide in the experimental conditions, which approximately equal to $100\% - \eta_{\text{ion-exchange}}$. The contributions of different interactions to the lead adsorption are shown in Figure 6. The results reveal that H$^+$/Pb^{2+} ion exchange is the dominant contribution to the lead adsorption at low pH (pH 2.0 and 3.0), which accounts for more than 70% of the whole adsorption capacity. Theoretically, the ion exchange increases with the elevation of pH value, and enhances the adsorption capacity caused by ion exchange, which is consistent with the experimental results in pH 2.0 to 3.0. Unexpectedly, the results are incompatible to the theoretical analysis in pH 3.0 to 4.0. It may be attributed to the involvement of the rapidly growing complexation interaction between Pb^{2+} and the functional groups in this pH range, which
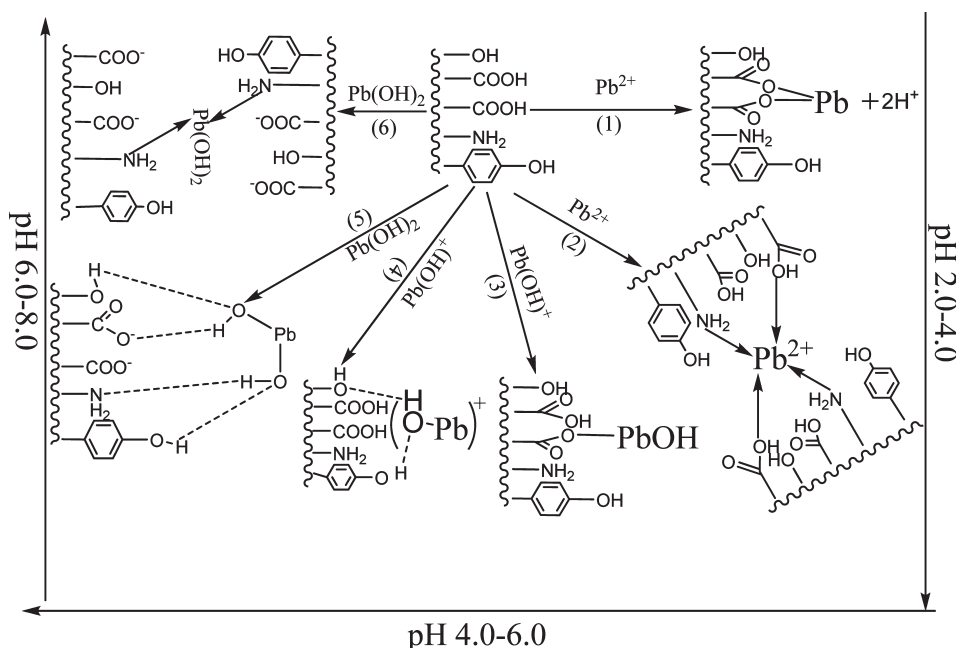
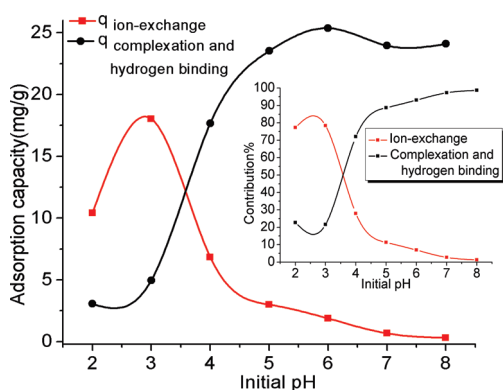**Figure 5.** Proposed mechanism for lead adsorption of *T. angustifoli*.

Figure 6. Estimation of the amount of lead adsorbed through different interactions. (inset figure) The contribution percentages of different interactions to the Pb adsorption. Adsorption conditions: contact time, 300 min; temperature, 298 K, initial lead concentration, 100 mg L^{-1}.

competes with the ion exchange interaction and results in decrease of ion exchange. As the pH increases from 4.0 to 8.0, because of the rapid decrease of protons and Pb^{2+} concentrations, the contribution of ion exchange between protons and Pb^{2+} to lead adsorption sharply reduces to 1.30%, which becomes almost negligible, while the complexation and hydrogen binding turn into dominant interactions.

On the basis of the analysis above, at pH 2.0−8.0, the proposed mechanism can interpret well our adsorption results (Figure 2) and those in the literature,[35,36] that is, the total adsorption capacity increases at pH 2.0− 6.0, and the slight decreases at pH 6.0−8.0, considering the three interactions between lead and the biomass.

4. CONCLUSIONS

T. angustifolia biomass was employed as an adsorbent to remove lead from aqueous solution. The adsorption isotherm is fitted to D-R model, and the maximum adsorption capacity is 123.8 mg g^{-1}. The SEM-EDX results indicate the lead is adsorbed on the surface of the biomass. FTIR characterization and the results of the blocking experiment verify the amino, hydroxyl, and carboxyl are the main functional groups contributing to the adsorption. The adsorption process is highly dependent on the pH, and pH 6.0 is the optimum pH, which can be well interpreted by the synergistic mechanism involving ion exchange, complexation, and hydrogen binding.

■ ASSOCIATED CONTENT

ⓢ Supporting Information. Additional characterizations of the adsorbent (surface area, pore volume and size (Table S1), Thermogravimetric analysis (Figure S1), N$_2$ adsorption−desorption isotherms (Figure S2)), and SEM-EDX analysis of the Pb-loaded biomass obtained at different solution pHs (Figure S3). This material is available free of charge via the Internet at http://pubs.acs.org.

■ AUTHOR INFORMATION

Corresponding Author
*E-mail: jhong@ustc.edu.cn. Phone: 86-551-3607482. Fax: 86-551-3607482.

■ ACKNOWLEDGMENT

■ REFERENCES

(1) Cheng, H.; Hu, Y. Lead (Pb) isotopic finger printing and its applications in lead pollution studies in China: A review. *Environ. Pollut. (Amsterdam, Neth.)* **2010**, *58*, 1134.

(2) Munagapati, V. S.; Yarramuthi, V.; Nadavala, S. K.; Alla, S. R.; Abburi, K. Biosorption of Cu(II), Cd(II) and Pb(II) by *Acacia leucocephala* bark powder: Kinetics, equilibrium and thermodynamics. *Chem. Eng. J.* **2010**, *157*, 357.

(3) ATSDR, Agency for toxic substances and disease registry. *Toxicological profile for lead*; ATSDR: Atlanta, GA, U.S.A., 2007.

(4) Southichak, B.; Nakano, K.; Nomura, M.; Chiba, N.; Nishimura, O. Phragmites australis: A novel biosorbent for the removal of heavy metals from aqueous solution. *Water Resour.* **2006**, *40*, 2295.

(5) Hasan, S. H.; Talat, M.; Rai, S. Sorption of cadmium and zinc from aqueous solutions by water hyacinth (*Eichchornia crassipes*). *Bioresour. Technol.* **2007**, *98*, 918.

(6) Alvarado, S.; Guédez, M.; Lué-Merú, M. P.; Nelson, G.; Alvaro, A.; Jesús, A. C.; Gyula, Z. Arsenic removal from waters by bioremediation with the aquatic plants Water Hyacinth (*Eichhornia crassipes*) and Lesser Duckweed (*Lemna minor*). *Bioresour. Technol.* **2008**, *99*, 8436.

(7) Mahamadi, C.; Nharingo, T. Competitive adsorption of Pb^{2+}, Cd^{2+} and Zn^{2+} ions onto *Eichhornia crassipes* in binary and ternary systems. *Bioresour. Technol.* **2010**, *101*, 859.

(8) Demirezen, D.; Aksoy, A. Accumulation of heavy metals in Typha angustifolia (L.) and *Potamogeton pectinatus* (L.) living in Sultan Marsh (Kayseri, Turkey). *Chemosphere* **2004**, *56*, 685.

(9) Koottatep, T.; Surinkul, N.; Polprasert, C.; Kamal, A. S. M.; Kone, D.; Montangero, A.; Heinss, U.; Strauss, M. Treatment of septage in constructed wetlands in tropical climate: lessons learnt from seven years of operation. *Water Sci. Technol.* **2005**, *51*, 119.

(10) Amon, J. P.; Abinash, A.; Shelley, M. L.; Opperman, B. C.; Enright, M. P.; Clemmer, N. D.; Slusser, T. L.; Jason, S.; Teresa, G.; William, E.; Andrew, C. Development of a wetland constructed for the treatment of groundwater contaminated by chlorinated ethenes. *Ecol. Eng.* **2007**, *30*, 51.

(11) Kantawanichkul, S.; Kladprasert, S.; Brix, H. Treatment of high-strength wastewater in tropical vertical flow constructed wetlands planted with *Typha angustifolia* and *Cyperus involucratus*. *Ecol. Eng.* **2009**, *35*, 238.

(12) Kuehn, K. A.; Suberkropp, K. Decomposition of standing litter of the fresh watere mergent macrophyte Juncus effusus. *Fresh Water Biol.* **1998**, *40*, 717.

(13) Longhi, D.; Bartoli, M.; Viaroli, P. Decomposition off our macrophytes in wetland sediments: Organic matter and nutrient decay and associated benthic processes. *Aquat. Bot.* **2008**, *89*, 303.

(14) Djebrouni, M.; Huon, A. Structure and biomass of a *Typha* stand revealed by multidimensional analysis. *Aquat. Bot.* **1988**, *30*, 331.

(15) Chubar, N.; Carvalho, J. R.; Correia, M. J. N. Cork biomass as a biomass for Cu (II), Zn (II) and Ni(II). *Colloids Surf., A* **2004**, *230*, 57.

(16) Das, S. K.; Das, A. R.; Guha, A. K. A study on the adsorption mechanism of mercury on *Aspergillus versicolor* biomass. *Environ. Sci. Technol.* **2007**, *41*, 8281.

(17) Iqbal, M.; Saeed, A.; Zafar, S. I. FTIR spectrophotometry, kinetics and adsorption isotherms modeling, ion exchange, and EDX analysis for understanding the mechanism of Cd^{2+} and Pb^{2+} removal by mango peel waste. *J. Hazard. Mater.* **2009**, *164*, 161.

(18) Yun, Y. S.; Volesky, B. Modeling of lithium interference in cadmium biosorption. *Environ. Sci. Technol.* **2003**, *37*, 3601.

(19) Chojnacka, K.; Chojnacki, A.; Goecka, H. Biosorption of Cr^{3+}, Cd^{2+} and Cu^{2+} ions by blue-green algae *Spirulina sp.*: kinetics, equilibrium and the mechanism of the process. *Chemosphere* **2008**, *59*, 75.

(20) Klika, Z.; Kraus, L.; Vopalka, D. Cesium uptake from aqueous solutions by bentonite: a comparison of multicomponent sorption with ion-exchange models. *Langmuir* **2006**, *23*, 1227.

(21) Schiewer, S.; Patil, S. B. Modeling the effect of pH on biosorption of heavy metals by citrus peels. *J. Hazard. Mater.* **2008**, *157*, 8.

(22) Farooq, U.; Kozinski, J. A.; Khan, M. A.; Athar, M. Biosorption of heavy metal ions using wheat based biosorbents - A review of the recent literature. *Bioresour. Technol.* **2010**, *101*, 5043.

(23) Fourest, E.; Volesky, B. Contribution of sulfonate groups and alginate to heavy metal biosorption by the dry biomass of *Sargassum fluitans*. *Environ. Sci. Technol.* **1995**, *30*, 277.

(24) Han, X.; Wong, Y. S.; Tam, N. F. Y. Surface complexation mechanism and modeling in Cr(III) biosorption by a microalgal isolate, *Chlorella miniata*. *J. Colloid Interface Sci.* **2010**, *303*, 365.

(25) Jeon, C.; Hol, W. H. Application of the surface complexation model to heavy metal sorption equilibria onto aminated chitosan. *Hydrometallurgy* **2004**, *71*, 421.

(26) Ngwenya, B. T.; Tourney, J.; Magennis, M.; Kapetas, L.; Olive, V. A surface complexation framework for predicting water purification through metal biosorption. *Desalination* **2009**, *248*, 344.

(27) Dubinin, M. M.; Radushkevich, L. V. Equation of the characteristic curve of activated charcoal. *Proc. Acad. Sci. U.S.S.R. Chem. Sec.* **1947**, *55*, 331.

(28) Hobson, J. P. Physical adsorption isotherms extending from ultrahigh vacuum to vapor pressure. *J. Phys. Chem.* **1969**, *73*, 2720.

(29) Uluozlu, O. D.; Sari, A.; Tuzen, M.; Soylak, M. Biosorption of Pb(II) and Cr(III) from aqueous solution by lichen (*Parmelina tiliaceae*) biomass. *Bioresour. Technol.* **2008**, *99*, 2972.

(30) Chen, J. P.; Yang, L. Chemical modification of *Sargassum sp.* for prevention of organic leaching and enhancement of uptake during metal biosorption. *Ind. Eng. Chem. Res.* **2005**, *44*, 9931.

(31) Chen, J. P.; Yang, L. Study of a heavy metal biosorption onto raw and chemically modified *Sargassum sp.* via spectroscopic and modeling analysis. *Langmuir* **2006**, *22*, 8906.

(32) Gardea-Torresdey, L. J.; Becker-Hapak, M. K.; Hosea, J. M.; Darnal, D. W. Effect of chemical modification of algal carboxyl groups on metal ion binding. *Environ. Sci. Technol.* **1990**, *24*, 1372.

(33) Giraldo, L.; Moreno-Pirajan, J. C. Pb^{2+} adsorption from aqueous solutions on activated carbons obtained from lignocellulosic residues. *Braz. J. Chem. Eng.* **2008**, *25*, 143.

(34) Nurchi, V. M.; Villaescusa, I. Agricultural biomasses as sorbents of some trace metals. *Coord. Chem. Rev.* **2008**, *252*, 1178.

(35) Kishore, K. K.; Meng, X. G.; Christodoulatos, C.; Boddu, V. M. Biosorption mechanism of nine different heavy metals onto biomatrix from rice husk. *J. Hazard. Mater.* **2008**, *153*, 1222.

(36) Subbaiah, M. V.; Vijaya, Y.; SivaKumar, N.; SubbaReddy, A.; Krishnaiah, A. Biosorption of nickel from aqueous solutions by *Acacia leucocephala* bark: Kinetics and equilibrium studies. *Colloids Surf., B* **2009**, *74*, 260.